



# Carbon – Science and Technology

ISSN 0974 – 0546

<http://www.applied-science-innovations.com>

ARTICLE

Received : 16/09/2014, Accepted : 21/10/2014.

---

## Thermodynamic study of the adsorption of chromium ions from aqueous solution on waste corn cobs material

Rafael A. Fonseca-Correa<sup>(A)</sup>, Marlon Bastidas-Barranco<sup>(B)</sup>, Liliana Giraldo<sup>(C)</sup>, Juan Carlos Moreno-Piraján<sup>(\*,A)</sup>

(A) Facultad de Ciencias, Departamento de Química, Grupo de Sólidos Porosos y Calorimetría, Universidad de los Andes, Colombia, Carrera 1 No 18 A 10, Bogotá, Colombia.

(B) Facultad de Ingeniería, Departamento de Ingeniería Mecánica, Universidad de la Guajira, Km 5 Via Maicao, Colombia.

(C) Facultad de Ciencias, Departamento de Química, Universidad Nacional de Colombia, Carrera 30 No 43-00, Bogotá, Colombia.

\* Author whom all correspondence: Prof.Dr. J.C. Moreno-Piraján, E-mail:jumoreno@uniandes.edu.co

The paper shows the results of a study obtaining activated carbon from corn cobs and determining its use as an adsorbent for the removal of  $\text{Cr}^{3+}$  from aqueous solutions. The finely ground precursor was subjected to pyrolysis at 600 and 900 °C in a nitrogen atmosphere and chemical activation with  $\text{H}_2\text{O}_2$  and  $\text{HNO}_3$ . The effects of pyrolysis conditions and activation method on the physicochemical properties of the materials obtained were tested. The samples were characterised chemically and texturally. Were obtained microporous activated carbons of well-developed surface area varying from 337 to 1213  $\text{m}^2/\text{g}$  and exhibited differences acid-base character of the surface. The results obtained shows that a suitable good option of the activation procedure for corncobs permits the production of economic adsorbents with high sorption capacity for  $\text{Cr}^{3+}$  from aqueous solutions. A detailed study of immersion calorimetry was performed with carbons prepared from corn cobs to establish possible relationships with these materials between the enthalpies of immersion and textural and chemical parameters.

**Keywords:** Waste corn cobs, Activated carbons, Pyrolysis, activation,  $\text{Cr}^{3+}$  removal, Immersion calorimetry, Enthalpy.

---

**1. Introduction:** The heavy metal pollution is of great interest about the effects they have on the human health hazards related with this kind type of contaminant. Due to their presence in environmental, these elements could be dissolved in water, be present in plants and animals, and finally in human across the food chain or by the consumption of contaminated water, causing serious damage [1, 2]. Non-treated waste water from industries such as leather tanneries, textile industries, stainless steel production, electroplating and metal finishing, etc., could contaminate water with chromium and other heavy metals. Chromium mainly exists in the environment in its hexavalent ( $\text{Cr}^{6+}$ ) and trivalent form ( $\text{Cr}^{3+}$ ). However it is well known that  $\text{Cr}^{3+}$  is less toxic than  $\text{Cr}^{6+}$ , prolonged exposure to  $\text{Cr}^{3+}$  species could also cause skin allergies and cancer in humans [3]. Also,  $\text{Cr}^{3+}$  can under certain conditions be oxidised to the state of more carcinogenic and mutagenic  $\text{Cr}^{6+}$  by some bacteria or manganese oxide present in the environment [2].

For a long time, it has been established by several authors in the literature [4] that the agricultural production and processing of agricultural products is related with the generation of large amounts of post-production wastes, such as corn cobs [5, 6], cotton stems [7], cherry stones [8], olive stones [9], grape stones [10], apricot stones [11, 12] orange peel [13, 14], etc. Properly remove waste, it is a work that are not normally perform well and in addition this involves collection, transportation and treatment end, which generates a cost, some communities prefer to discard no treat it generating a serious environmental problem [15 - 19]. In Colombia, 80 % of the national corn cobs production is destined for human consumption and the remnant 20% is used in the feed industry. Consumption for 2012 was four million tons. The corn cob as a by-product of corn is given various domestic, craft uses food for some animal or as fuel [18, 19]. In recent years it has invested in research to obtain activated carbon from this residue [2, 16-18 ].

These carbons have certain advantages over the raw material like the high porosity is developed a surface area close to one thousand square meters per gram of activated carbons characteristic [17, 19]. Another great advantage is that these materials have different chemical surface functional groups developed during its production process, which make them useful for various applications [2].

Moreover, characterization of microporous adsorbents by immersion calorimetry is not as straightforward as in the case of non-porous adsorbents. Atkins et al. [20] measured the heats of immersion of a microporous carbon cloth and a microporous activated carbon in a series of organic liquids and, for a given solid, they obtained a great dependence of the heat of immersion with the liquid used. They concluded that the heat of immersion is a measure of the volume of pores accessible to the molecule of the immersing liquid, thus opening the possibility of using immersion calorimetry as a tool to obtain pore size distribution in microporous carbons.

The purpose of this research was to obtain carbonaceous adsorbents from corn cobs pyrolysis and chemical activation, studying the relationships between heats of immersion and different textural and chemical properties of these porous solids and their application in adsorption of  $\text{Cr}^{3+}$  in aqueous solutions.

## **2. Experimental:**

**2.1 Preparation of activated carbons:** The initial corncobs (TMO) were grinded into particles of approximately 2 mm in size and were subjected to pyrolysis [21]. This process was carried out in a horizontal furnace under nitrogen atmosphere. The laboratory assembly for the carbonising process is shown in Figure (1) [22]. A quartz glass tube was used as a reactor. The diameter and length of the fluidised bed reactor in the bed section were 10 cm and 50 cm, respectively. One quartz boat, with holes in its base for the diffusion of nitrogen and 10 cm in length, was placed along with the material, which was previously weighed, in the centre of the reactor. The  $\text{N}_2$  was introduce into the bed through a pressure regulator (10 mL/min flow) and a heating furnace controlled by a programmable thermostat, which was heating at a rate of 10 °C/min. The reactor was first heated to the present temperature and then maintained until thermal equilibrium was achieved.



Figure (1): Set up for carbonisation and the activation of corncobs: Parts a) Nitrogen gas and Oxygen gas, b) Feed valves, c) Gas Flowmeter, d) Reactor, e) Sample holder, f) Furnace, g) Gas cleaning filter system, h) Gases to vent.

The sample of started (TMO) was heated (10 °C/min) from room temperature to the final pyrolysis temperature of 600 °C (TM600) and 900 °C (TM900). Samples were kept at the final pyrolysis temperature for 240 min and then cooled down. The products of pyrolysis were next subjected to chemical activation (TMC). Chemical activation by H<sub>2</sub>O<sub>2</sub> (35 %) H<sub>2</sub>SO<sub>4</sub> (98 %) and HNO<sub>3</sub> (65 %) H<sub>3</sub>PO<sub>4</sub> (85 %) was performed with an acid/char weight ratio of 2/1 for 30 min, in nitrogen atmosphere (flow rate 10 mL/min) at 600 °C and 900 °C. These samples were labelled as: TMCP600, TMCP900, TMCN600 and TMCN900.

**2.2. Analytical procedures:** The elemental analysis of the starting corn cobs, chars and activated carbons were performed on an elemental analyser CHNS Perkin Elmer AD 6000 (USA). TG was performed using a Netzsch STA 409 (Germany) under the nitrogen (5mL/min) atmosphere at a heating rate of 1°C/min.

The specific surface area and porosities of samples for activated carbon were determined by nitrogen gas adsorption-desorption at –196 °C using a Quantachrome Autosorb Automated Gas Sorption System IQ<sub>2</sub> (Quantachrome Corporation USA). The nitrogen adsorption-desorption isotherms of activated carbon were obtained by calculating their Brunauer-Emmett-Teller (BET) surface areas by assuming that the area of the N<sub>2</sub> molecule was 0.162 nm<sup>2</sup>. The BET surface area was assessed within the range of relative pressures from 0.05 to 0.3. The micropore volume and external surface area (mesoporous surface area) were measured by t-plot method [23]. The total pore volume was calculated by measuring the amount of N<sub>2</sub> adsorbed at a relative pressure of 0.99. The Horvath and Kawazoe (HK) method [24] for micropore size distribution was used for characterisation of the carbon. The Barrett-Joyner-Halenda (BJH) method [25] was used for the pore size distribution of the result carbon in the mesoporic range.

The pH of activated carbons and chars was measured using the following procedure: a portion of 1.0 g of dry activated carbon powder and chars was added to 10 mL of distilled water and the suspension was stirred to reach equilibrium. The pH of the suspension was measured at 25 °C.

**2.3. pH Study:** Measurements of the effects of various pH on the adsorbent performance used 0.1 g of each adsorbent (samples of porous solids prepared) added to 50 mL of  $50 \mu\text{g L}^{-1} \text{Cr}^{3+}$  solution. The various pH solutions were prepared by adding dilute NaOH or  $\text{HNO}_3$  dropwise to achieve pH values of 2.0 through 12.0. Bottles were shaken at 125 rpm for 48 h at constant temperature ( $25.0 \pm 1^\circ\text{C}$ ).

**2.4 Determination of basic and acidic oxygenated groups by the Boehm method:** Boehm's method [26] was used to determine the total acid oxygenated groups, starting from 0.5 g. Each of the carbons were contacted for 24 h. at room temperature with 50 mL of 0.1 M NaOH solution. Then the carbon was filtered and the solution was titrated potentiometrically with a 0.1 M HCl solution to determine the amount of NaOH consumed. For basic oxygenated groups, the above procedure was repeated using 0.1 M HCl, then titrate the excess with a 0.1 M NaOH solution.

**2.5. Adsorption isotherm:** In order to evaluate the  $\text{Cr}^{3+}$  removal capacity on samples prepared in this research, batch equilibrium tests were conducted. The solutions are set to a pH of 4.8. A given mass of corn cob was added to a Nylon mesh basket and then placed inside the adsorber solution [20]. The corn cob doses used were between 0.15 - 1.50 g, and the initial concentrations of  $\text{Cr}^{3+}$  varied from 10 to 600 mg/L. The adsorber was maintained at constant temperature and was continuously stirred. All solutions were prepared with analytical grade reagents, using chromium nitrate (Merck,USA) and deionized water.

The solution of  $\text{Cr}^{3+}$  and corn cob remained in contact until equilibrium was achieved. The pH solution was measured periodically with a pH meter and kept constant by adding 0.01 M  $\text{HNO}_3$  and NaOH solutions as required. Samples were taken at various times and the  $\text{Cr}^{3+}$  concentration of each sample was determined as described below. Once the concentration of  $\text{Cr}^{3+}$  in two subsequent samples showed no significant variation between them it was considered that equilibrium had been achieved. Preliminary experiments showed that 15 days was enough to reach equilibrium. The  $\text{Cr}^{3+}$  uptake was calculated by performing a mass balance.

The concentration of  $\text{Cr}^{3+}$  in aqueous solutions was determined by atomic absorption spectroscopy using a Varian, double beam, atomic absorption spectrophotometer, model SpectrAA-20 [19]. The  $\text{Cr}^{3+}$  concentration of a sample was estimated using a calibration curve (concentration versus absorbance), which was prepared using standard concentration Cr(III) solutions. Percentage removal (R, %) was calculated according to the following equation:

$$R = \frac{C_o - C_e}{C_e} \times 100 \quad (1)$$

where R is the percentage removal of  $\text{Cr}^{3+}$ , and  $C_o$  and  $C_e$  are the initial and residual concentrations ( $\text{mg}\cdot\text{L}^{-1}$ ) of  $\text{Cr}^{3+}$ , respectively. Adsorption isotherms were obtained with different initial concentrations of  $\text{Cr}^{3+}$ , while the initial weight of activated carbons corncobs remained constant. In order to correct a potential adsorption  $\text{Cr}^{3+}$  in the surface of the container, the control experiments were carried out in the absence of activated carbon. In all experiments, the difference between the initial concentration of  $\text{Cr}^{3+}$  ( $C_o$ ) and the equilibrium concentration ( $C_e$ ) was calculated and used to determine the adsorption capacity ( $q_e$ ) by the following equation:

$$q_e = \frac{V}{m} (C_o - C_e) \quad (2)$$

where V is the total volume of the solution of  $\text{Cr}^{3+}$ , m is the mass of adsorbent (g),  $C_o$  is the initial concentration of  $\text{Cr}^{3+}$  ( $\text{mg}\cdot\text{L}^{-1}$ ), and the balance  $C_e$   $\text{Cr}^{3+}$  ( $\text{mg}\cdot\text{L}^{-1}$ ). The linear model that describes the

accumulation a solute in an adsorbent, is directly proportional to the concentration in the solution, and is represented by the equation:

$$q_e = K_D C_e \quad (3)$$

The constant of proportionality or distribution coefficient  $K_D$  is often referred to as the partition coefficient.

Langmuir model represents one of the first theoretical treatments applied to nonlinear adsorption in a wide range of systems to limit maximum adsorption capacity due to saturated adsorbate molecules on the adsorbent surface monolayer. In this model, all sites have the same adsorption activation energy of adsorption. The Langmuir equation can be written as:

$$q_e = \frac{Q^o b C_e}{1 + b C_e} \quad (4)$$

where  $Q^o$  and  $b$  are constants related to the adsorption capacity and adsorption energy, respectively. The linear form of the Langmuir equation can be represented as follows:

$$\frac{1}{q_e} = \frac{1}{Q^o} + \frac{1}{b Q^o} \frac{1}{C_e} \quad (5)$$

Equation (3) is also used to analyse the equilibrium data in batch by plotting  $1/q_e$  versus  $1/C_e$ , reproducing a linear trend if the data fit the Langmuir isotherm.

The Freundlich isotherm adsorption is assumed to produce a heterogeneous surface, through an adsorption mechanism in multiple layers, and that the adsorbed amount increases with the concentration in accordance with:

$$q_e = K_F C_e^{1/n} \quad (6)$$

where  $K_F$  is the Freundlich constant related to the adsorption capacity (mg/g, mg/L),  $C_e$  is the concentration of the adsorbate in the solution at equilibrium (mg/L),  $n$  is an empirical parameter representing energy heterogeneity adsorption sites (dimensionless). The logarithmic form of equation (6) below is used typically for adjusting the data batch equilibrium studies:

$$\log q_e = \log K_F + \frac{1}{n} \log C_e \quad (7)$$

**2.6. Immersion enthalpy:** The immersion enthalpies of the corn cob activated carbon were determined in nitrate solutions of  $\text{Cr}^{3+}$  of different concentrations ranging between 20 and 100 mg L<sup>-1</sup> for the maximum adsorption at pH = 6.0, in a homemade immersion microcalorimeter [22], see Figure (2).

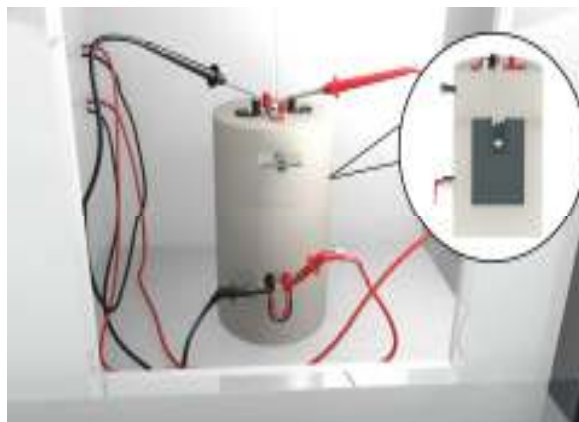


**Figure (2): Immersion microcalorimeter for the determination of solid-liquid enthalpy interactions.**

The immersion enthalpies were also determined for solutions of  $100 \text{ mg L}^{-1}$  up to the pH values selected. To perform this determination, a heat conduction microcalorimeter was used with a stainless steel calorimetric cell. The temperature of 30 mL of the solution was raised to  $25^\circ\text{C}$ ; this was then placed in the cell. A sample of activated carbon of approximately 0.5 g was weighed and placed inside the calorimetric cell in a glass ampoule. The microcalorimeter is then assembled. When the equipment reached a temperature of about  $25^\circ\text{C}$ , the potential readings began after a period of approximately 15 minutes, with readings every 20 seconds; the glass ampoule was broken and the thermal effect generated was registered. The potential readings continue for approximately 15 minutes more and at the end of the experience.

**Table (1): Elemental analysis of corn cobs, chars and activated carbons obtained and the yield of pyrolysis and activation processes (wt%)**

Sample	Ash	VM*	C <sup>dat**</sup>	H <sup>dat</sup>	N <sup>dat</sup>	O <sup>dat***</sup>	Yield
TMO	1.0	58.7	44.5	5.3	1.09	49.08	--
TM600	2.5	21.3	74.5	3.9	0.67	10.54	--
TM900	5.6	15.7	77.5	2.2	0.45	12.5	--
TMCP600	0.9	--	85.2	1.5	0.67	10.8	--
TMCP900	0.7	--	96.3	1.1	0.51	6.7	--
TMCN600	0.6	--	81.9	1.0	0.48	9.8	--
TMCN900	0.4	--	90.3	0.6	0.39	7.9	--

(A<sup>d</sup>):Ash by difference; \* volatile matter; \*\* dry-ash-free basis; \*\*\* determined by difference.

### 3. Results and discussions:

**3.1 Elemental composition of the chars and activated carbons:** As corn cobs are characterised by very low content of carbon and high content of volatiles, Table 1, they were first subjected to pyrolysis at different temperatures. The products of pyrolysis were chars TM600 and TM900, characterised by much higher carbon content; the content of the ashes was slightly higher but there was a much lower

content of volatiles than the initial material. Changes in the above contents significantly depended on the temperature of pyrolysis and were much more pronounced for the TM900 sample.

Further analysis of the data from Table (1) indicates that, irrespective of the variant used, the process of activation led to further changes in the structure of carbonaceous material. The products of activation, in particular those obtained from char

TM900, were characterised by a greater contribution of carbon and much lower content of  $H^{daf}$  than the corresponding chars. The content of oxygen in the activated carbons changes in a different way: in samples TMCP600 and TMCN600, obtained by activation with sulphuric and phosphoric acids of char TM600 and TM900, respectively, the content of oxygen was higher, while in samples TMCN900 and TMCP900 it was slightly lower. The content of nitrogen was different in the products of pyrolysis. An important feature was a very low content of ashes in the activated carbon samples obtained ( $A^d$ ).

**3.2 TGA, proximate and ultimate analysis:** The carbonization profile of the samples of the corn cobs, Fig. 3, indicates no significant changes in weight to 200 °C. Fast switching between 200–400 °C. These are typical behaviors of lignocellulosic materials are then produced. Such a profile has been observed in several carbonizing carbonaceous materials, such as sawdust and onion skin [27], iron bamboo [28] and palm shell [29], which had not been mixed with inorganic activating agents. Lignocellulosic materials corncobs consist of three major components: cellulose, hemicellulose and lignin.

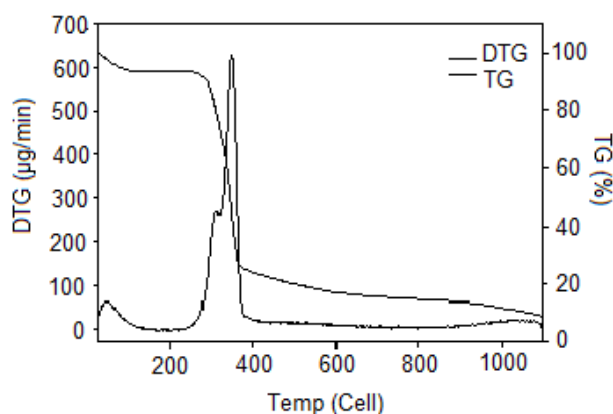


Figure (3): TGA-DTG profiles of the corn cob precursor of activated carbon heated at 2°C/min in nitrogen atmosphere.

Above 400 °C, decomposition occurs by depolymerisation and scission of polymer chains involving ether bonds and carbon-carbon. As obtained in the TGA, Figure (2), an initial rapid change in the decomposition of the hemicellulose can be seen, continuous with the lignin. In addition, during this process, cellulose units, which are the main component of plant materials are subjected to depolymerisation and start to become smaller units, enriching the solid matter in carbon [30].

**3.3 Textural parameters of chars and activated carbons:** As follows from the data presented in Table (2), the carbon samples obtained by the chemical activation of corn cobs show a variety of textural parameters, depending considerably on the temperature of pyrolysis and the variant of activation. The surface areas of carbons obtained by the pyrolysis of corn cobs and activated by chemical methods were 456 and 1345 m<sup>2</sup>/g, respectively, while their pore volumes were 0.23 and 0.78 cm<sup>3</sup>/g, respectively.

As expected, with the chemical activation, development of a porous structure is high. The samples obtained in this way were characterised by 3-5 times larger surface area and total pore volume than those activated by simple pyrolysis or in respect to the original sample.

As mentioned above, the temperature of pyrolysis also affected the parameters of carbon samples activated by  $H_2O_2$  or  $HNO_3$ . For the samples obtained by chemical activation, the higher the pyrolysis temperature, the less developed the porous structure; this is probably due to the high temperature part of the structure collapsing, meaning that the area decreases. All of the activated carbon samples have a microporous structure, as the contribution of micropores in the total pore volume varies in the range 86–97 %. The other pores are mesopores of diameters varying in the range 2.00–2.58 nm.

Table (2): Textural characteristics of the different samples prepared deduced from  $N_2$  adsorption isotherms at  $-196\text{ }^\circ\text{C}$  and  $CO_2$  adsorption isotherms at  $0\text{ }^\circ\text{C}$  respectively.

Sample	$S_{BET}$ ( $m^2.g^{-1}$ )	$V_0$ ( $cm^3.g^{-1}$ )	$V_{meso}$ ( $cm^3.g^{-1}$ )	$V_t$ ( $cm^3.g^{-1}$ )	Average Pore diameter (nm)	External Surface Area ( $m^2.g^{-1}$ )
TMO	436	0.29	0.09	0.38	2.20	89
TMCP600	885	0.42	0.11	0.53	2.00	155
TMCP900	995	0.49	0.14	0.63	2.37	194
TMCN600	1115	0.51	0.17	0.68	2.51	217
TMCN900	1345	0.59	0.20	0.79	2.58	245
TM900	534	0.34	0.23	0.57	2.15	120

$S_{BET}$ : “Apparent” surface area calculated using the BET;  $V_0$ : Micropore volumen calculated by applying the t-plot method;  $V_t$ : Total pore volume obtained from the amount of  $N_2$  adsorbed at  $P/P^0 \approx 0.95$ ;  $V_{meso}$ : Mesopore volume obtained by Barrett-Joyner-Halenda,  $V_t$  from  $V_0$ ; external surface area calculaed by t-plot method.

**3.4 Acid-base properties of the chars and activated carbons:** According to the data presented in Table (3), the acid-base properties of the adsorbents are very different. The pH of the samples varied from 4.6 to 6.2, while the content of oxygen surface groups varied from 0.66 to 3.03 mmol/g. The samples obtained by chemical activation with sulphuric and phosphoric acids have acidic surfaces, with pH close to 4.5. The adsorbents differ not only in the amount of surface oxygen groups but also in their type. Two samples TMCN600 and TMCN900 have surfaces with dominant presence of acidic groups, while samples TMO is basic and TMCP600 and TMCP900 have surfaces with groups who generate a slightly acid pH, which is lower compared to other samples.

Thus, the type and number of surface oxygen groups depends first of all on the variant of activation and the temperature of pyrolysis of the initial material. The highest total content of surface functional groups was observed for the samples obtained by chemical activation of both chars, while the lowest was for

crude sample, TMO. The increase in temperature of pyrolysis from 600 °C to 900 °C favours the generation of a greater number of acidic groups. The temperature of pyrolysis also influences the amount of functional groups in the products of activation, which follows from the fact that all samples obtained from the activation of char TMCN900 have a smaller number of basic groups and a greater number of acid character groups than analogous adsorbents obtained from char TMCN600.

**3.5 Analysis of the calorimetric results in function the of textural properties:** Figure (4) includes plots for the surface area of some activated carbons, as determined by immersion calorimetry into dichloromethane, benzene and 2,2-dimethylbutane, as a function of the minimum molecular dimension of the liquid.

Table (3): Acid base properties of the chars and activated carbons obtained

Sample	pH	Acidic Groups (mmol/g)	Basic Groups (mmol/g)	Total content of surfaces oxides (mmol/g)
TMO	6.2	0.00	0.66	0.66
TM600	5.8	1.78	0.56	2.34
TM900	5.5	1.84	0.41	2.25
TMCP600	5.2	1.95	0.32	2.27
TMCP900	5.0	2.34	0.21	2.55
TMCN600	4.8	2.68	0.14	2.82
TMCN900	4.6	2.95	0.08	3.03

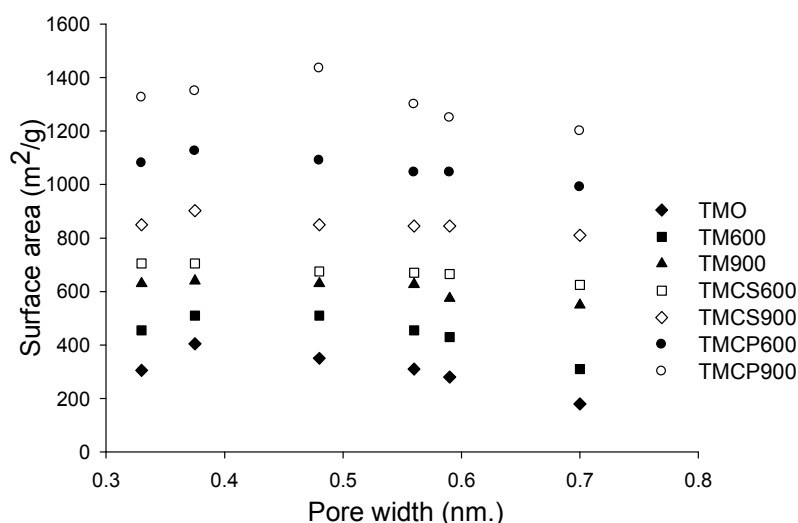


Figure (4): Surface area ( $\text{m}^2/\text{g}$ ) for different activated carbons prepared into liquids of different molecular dimensions: dichloromethane (DMC), benzene (BZ), cyclohexane, 2,2-dimethyl-butane (DMB) and  $\alpha$ -pinene.

Figure (4) shows the surface area of a series of carbon samples as a function of pore width. This pore width was calculated from the molecular dimensions of the various immersion liquids used. It can be seen that a distinct cut-off point is observed for the samples TMO, TM600 and TM900 just before 0.38 nm, which probably indicates that there is a narrow pore size distribution for these samples. These samples, however, seem to show a rather larger pore size distribution in the micropore range, whereas the other samples seem to consist of pores with larger dimensions.

The advantage of the use of the calorimetric method for the estimation of micropore surface areas lies in the fact that the energy released upon immersion is directly proportional to the interaction surface. This is an advantage with respect to the BET method, in which the number of molecules which form a statistical monolayer is multiplied by the cross-sectional area of the molecules, and can lead to underestimation and overestimation of ultramicropore and supermicropore surface areas, respectively. This was not the case for immersion calorimetry, in which the immersion energy was proportional to the area of interaction with the surface. Thus, for example, the immersion energy of a molecule inside a cylindrical ultramicropore is a 3.6 times greater than on an open surface.

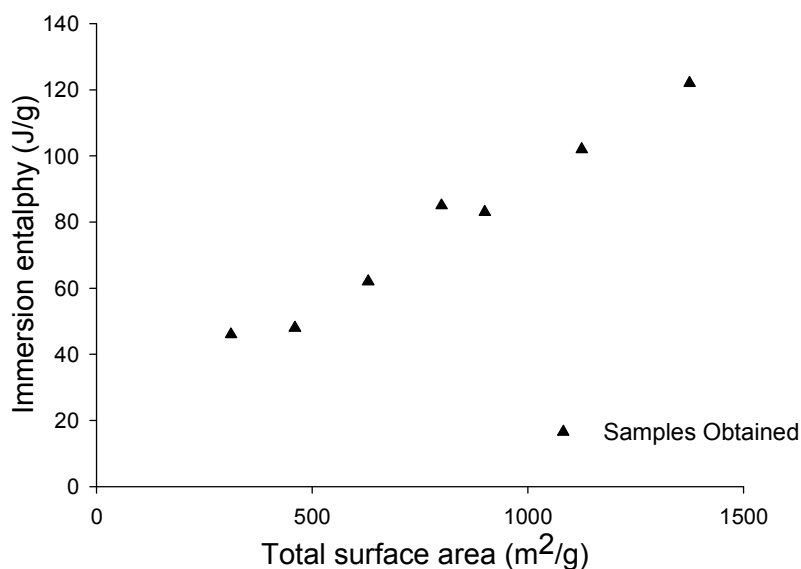


Figure (5): Immersion enthalpies (J/g) in function of total area (m<sup>2</sup>/g) of samples researched using benzene: Sample TMCN900.

The results obtained for the immersion enthalpies showed that there is a linear relationship between the enthalpies of immersion in benzene and areas for different samples calculated from the Stoekli-Krahenbuhl equation. This can be seen in Figure (5) showing the immersion enthalpies sample benzene TMCN900. The results are in good agreement with those reported in the literature and in works published by our research group. Here, this accessibility recorded benzene molecules in the porous structure of each of the samples prepared in this work. It should be noted that the areas obtained were very close to those obtained experimentally by the N<sub>2</sub> adsorption isotherms at -196°C.

Figure (6) shows the relationship between immersion enthalpies in benzene and the average pore diameter of the different samples prepared in this work. It can be seen that the enthalpy of immersion in benzene presents low value in samples where the average pore diameter is smaller, as in the case of TM900 and TMCP900. In contrast, the highest values of enthalpies correspond to samples TMCN600 and TMCN900, and these results agree with those found in this work for the relationships studied.

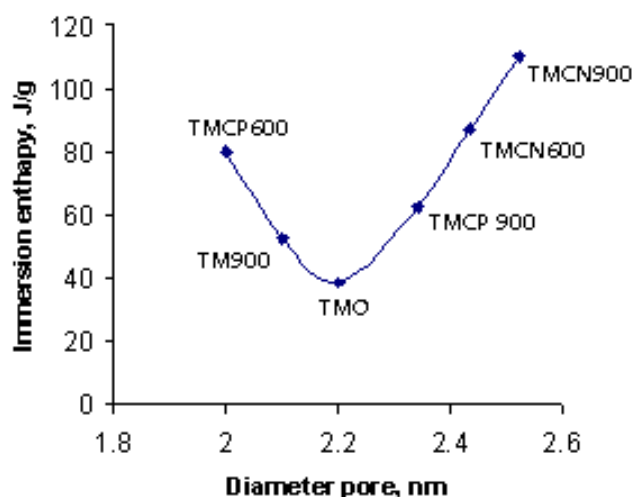


Figure (6): Enthalpies of immersion (J/g) for different activated carbons prepared into benzene versus diameter pore.

In the absence of specific interactions at the solid-liquid interface, immersion calorimetry into liquids of different molecular dimensions can be used to estimate the total surface accessible for a given molecule. As can be observed (data not shown here) a small molecule such as dichloromethane, with a kinetic diameter of 0.33 nm (similar to nitrogen; 0.36 nm) is able to access the entire porosity on both samples (TMCN600 and TMCN900), giving rise to a large enthalpy value (~125 J/g). However, a molecule with a slightly higher diameter, such as benzene, exhibits important restrictions, i.e. there is a sudden decrease in the heat of interaction, with these effects being more drastic for samples such as TMCP600 and TMCP900. Finally, 2,2-dimethyl-butane and  $\alpha$ -pinene, with a kinetic diameter of 0.56 nm and 0.70 nm, respectively, are unable to access the porous structure in both samples. These results constitute an empirical prove of the molecular sieve effect on the activated carbon materials prepared in this work. According to the calorimetric measurements, the pore size opening on both samples must be below 0.56 nm, with this value being slightly lower for samples mentioned before, i.e. a narrower micropore entrance on this samples compared with the others samples prepared.

**3.7. Analysis of the results of the isotherms from aqueous solution:** The adsorption isotherms are critical to evaluate the ability of adsorption of porous solids. They also provide an overview of the studio system, how will the efficiency of activated carbons obtained from the corn cobs and can estimate an economic feasibility with regard to the applications these carbons have certain specific solutes, for our case  $\text{Cr}^{3+}$ .

In order to fit the experimental data to theoretical models appropriate adjustment results, we have considered the Langmuir equation and Freundlich (Equations 4 and 6). These results are shown in Figure (7) and in Table (4).

Activated carbons obtained at different activation times shown adequate adsorption capacity for Cr (III) (TMCP600, TMCP900, TMCN600 y TMCN900). The regression coefficients ( $R^2$ ) of Langmuir all synthesized materials were between 0.9999 and 0.9981, suggesting that the adsorption of Cr (III) on activated carbon corn cobs can be well explained by the model, suggesting that the adsorption filling is monolayer [30-32].

The  $q_m$  values are shown in Table 4.

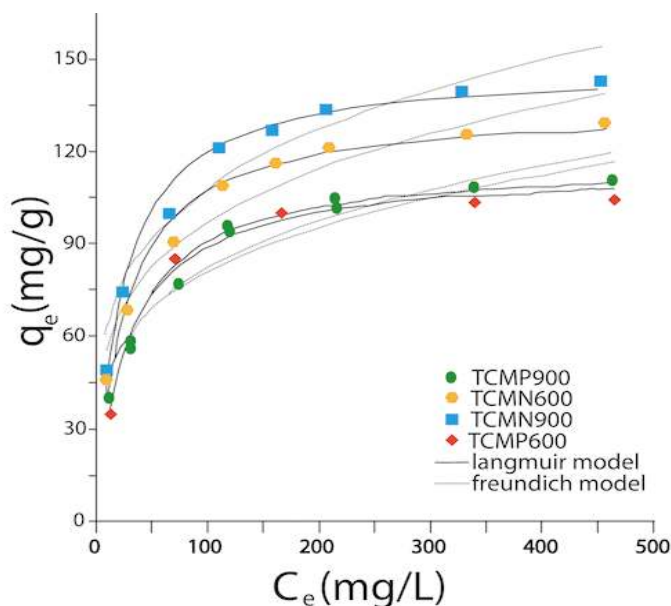


Figure (7): Adsorption of chromium – Freundlich and Langmuir models.  
Conditions: pH: 4.5, Temp: 25°C.

Figure (7) shows that the maximum adsorbed amount of  $\text{Cr}^{3+}$  on activated carbons is synthesized with 132.54 mg/g for TMCN900 at pH 4.5. The effect of degree of modification on the adsorption capacity of the activated carbon obtained from eargopher (TMCP600, TMCP900 TMCN600 and TMCN900), was investigated by determining the adsorption isotherms of  $\text{Cr}^{3+}$  at pH = 4.5 and T = 25 °C. The experimental data of adsorption equilibrium and the representation of adsorption isotherms are shown in Figure (7). It can be seen that the adsorption capacities of the activated carbons are dependent on the degree of thermal modification. The adsorption capacity increased with progressively higher activation time. Solid lines ( \_\_\_ ) represents the isotherms the Langmuir and dashed lines ( ---- ) represent Freundlich. Thus, the maximum adsorption capacity decreases in the order:

$$\text{TMCN900} > \text{TMCN600} > \text{TMCP900} > \text{TMCP600}$$

Table (4): Isotherm model constants and correlation coefficients for adsorption of  $\text{Cr}^{3+}$  ions onto activated carbon activated chemically from corn cob, at pH=4.5 and T= 25°C.

	Langmuir			Freundlich		
	$q_e$	K	$R^2$	$K_F$	n	$R^2$
TMCP600	66.78	0.0437	0.9999	18.213	1.654	0.9843
TMCP900	79.67	0.0264	0.9987	21.231	2.654	0.9654
TMCN600	104.51	0.0859	0.9981	30.321	2.875	0.9798
TMCN900	132.54	0.2341	0.9983	41.654	2.986	0.9852

This observed variation in descending order in the same way that the concentration of oxygenated carboxylic acid groups, determined by titration Boehm selective (not shown here). Therefore, the adsorption capacity is dependent on the carboxyl sites, and the adsorption capacity is proportional to the concentration of both carboxyl sites, and the total concentration of acid sites. It is assumed that the

adsorption capacity is more dependent on the concentration of carboxylic hydroxyl sites of the sites (the presence of these are very low). This assumption is based on the fact that in the modification by heat treatment, the concentration of carboxylic sites increased more significantly than that of the hydroxyl sites, and most deprotonated carboxylic sites on the experimental pH (4.5)

**4. Conclusions:** Activated carbon and porous solids were obtained from corn cob using different activation methods and activators. Among them, the carbon produced by treatment with 4 hours of activation yielded the largest BET-specific surface area and total pore volume, namely 1345 m<sup>2</sup>/g and 0.78 cm<sup>3</sup>/g respectively. All carbons prepared in this research present a microporous character. The TMCN900 sample showed the highest amount of chromium adsorbed, and the lowest capacity of adsorption was presented by TMCP600.

This research shows that porous solids obtained from raw corn cobs are useful in the adsorption of trivalent chromium under the experimental conditions of this work. The adsorption of Cr<sup>3+</sup> onto ACs is adjusted to the Langmuir model.

**ACKNOWLEDGEMENTS:** The authors are grateful for the convenio marco between the Universidad de los Andes (Colombia, South America) and the Universidad Nacional de Colombia and also the Proyecto Semilla de la Facultad de Ciencias of the Universidad de los Andes, for the funding partial of this research.

## 5. References:

- [1] J. Li, Q. Lin, X. Zhang, Y. Yan, Y. J. Colloid Interf. Sci. 333 (2009) 71.
- [2] R. B. Garcia-Reyes, J. R. Rangel-Mendez, Bioresour. Technol. 101 (2010) 8099.
- [3] Y. S. Yun, D. Park, J. M. Park, B. Volesky, Environ. Sci. Technol. 35 (2001) 4353.
- [4] J. Kazierczak, P. Nowicki, P. Pietrzak, Adsorption 19 (2013) 273.
- [5] M. Song, B. Jin, R. Xiao, L. Yang, Y. Wu, Z. Zhong, Y. Huang, Biomass and bioenergy 48 (2013) 250.
- [6] S. Nethaji, A. Sivasamy, A. B. Mandal, Bioresource Technology 134 (2013) 94.
- [7] N. Anas, M. Nail, P. T. Williams, Biomass and bioenergy 37 (2013) 142.
- [8] R. Pietrzaka, P. Nowickia, J. Kazmierczaka, I. Kuszynskaa, J. Goscianskaa, J. Przepiórski, Chemical Engineering Research and Design 2013; Article in Press. No. of pages 5.
- [9] M. Tamer, I. Abustan, A. Azmier, M. Ahmad, J. of Env. Chem. Eng. 1 (2013) 589.
- [10] D. Jimenez-Cordero, F. Heras, N. Alonso-Morales, M. A. Gilarranz, J. J. Rodriguez, Biomass and Bioenergy 54 (2013) 123.
- [11] I. Tsibranska, E. Hristova, Chemical Engineering and Processing 49 (2010) 1122.
- [12] L. Mouni, D. Merabet, A. Bouzaza, L. Belkhiri, Desalination 276 (2011) 148.
- [13] V. K. Gupta, A. Nayak, Chemical Engineering Journal 180 (2012) 81.
- [14] M. Torab-Mostaedi, M. Asadollahzadeh, A. Hemmati, A. Khosravi, Journal of the Taiwan Institute of Chemical Engineers 44 (2013) 295.
- [15] W. T. Tsai, C. Y. Chang, S. Y. Wang, S. F. Chang, C. F. Chien, H. F. Sun, Resour. Conserv. Recycl. 32 (2001) 43.
- [16] C. F. Chang, C. Y. Chang, W. T. Tsai, J. Colloid Interface Sci. 232 (2000) 45.
- [17] N. V. Sych, S. I. Trofymenko, O. I. Poddubnaya, M. M. Tsyba, V. I. Sapsay, D. O. Klymchuk, A. M. Puziy, Appl. Surf. Sci. 261 (2012) 75.
- [18] W. T. Tsai, C. Y. Chang, S. L. Lee, Bioresour. Technol. 64 (1998) 211.
- [19] M. Sevilla, A. B. Fuertes, R. Mokaya, Int. J. Hydrog. Energy 36 (2011) 15658.
- [20] D. Atkins, A. I. McLeod, K. S. W. Sing, A. Capon, Carbon 20 (1982) 339.
- [21] R. A. Fonseca-Correa, L. Giraldo, J. C. Moreno-Piraján, J. Anal. Appl. Pyrol. 101 (2013) 132.

- [22] J. C. Moreno-Piraján, R. Gómez-Cruz, V. García-Cuello, L. Giraldo, J. of Anal. and Appl. Pyrol. 89 (2010) 122.
- [23] B. C. Lippens, J. H. de Boer, J. Catal. 4 (1965) 319.
- [24] G. Horvath, K. Kawazoe, J. Chem. Eng. Jpn. 16 (1983) 470.
- [25] E-P. Barret, L. G. Joyner, P. H. Halenda, J. Am. Chem. Soc. 73 (1951) 373.
- [26] H. P. Boehm, E. Diehl, W. Heck, R. Sappok, Angew. Chem., Int. Ed. Engl. 3 (1964) 669.
- [27] T. O. Odozi, S. Okeke, R. B. Lartey, Agricult. Wastes 12 (1985) 13.
- [28] R. Zhang, B. Wang, H. Ma, Desalination. 255 (2010) 61.
- [29] T. Odozi, R. Emelike, J. of Appl. Polym. Sci. 30 (1985) 2715.
- [30] M. S. Azab, P. J. Peterson, Water Sci. Technol. 21 (1989) 1705.
- [31] D. I. Rai, B. M. Sass, D. A. Moore, D. A., Inorg. Chem. 26 (1987) 345.
- [32] C. Moreno-Castilla, C. A. Álvarez-Merino, L. M. Pastrana-Martínez, M. V. López-Ramón, J. Colloid Inter. Sci. 345 (2010) 461.

\*\*\*